IEEE Access
Multidisciplinary | Rapid Review | Open Access Journal

Received December 30, 2021, accepted January 10, 2022, date of publication January 14, 2022, date of current version January 24, 2022.

Digital Object Identifier 10.1109/ACCESS.2022.3143807

Automated Lane Change Featuring Re-Planning in Dynamic Environments and Sensitivity Analysis of Main Operational Parameters

CORNELIA LEX, DEMIN NALIC, (Member, IEEE), SAJJAD SAMIEE, AND ARNO EICHBERGER
Institute of Automotive Engineering, Graz University of Technology, 8010 Graz, Austria

Corresponding author: Cornelia Lex (cornelia.lex@tugraz.at)

This work was supported by the Austrian Federal Ministry of Transport, Innovation and Technology as part of the Österreichische Forschungsförderungsgesellschaft (FFG) Project EFREtop.

ABSTRACT Lane changes are frequent maneuvers in everyday driving and have to be included in automated driving functions. We present a real-time capable implementation of an algorithm for an automated lane change with the capability of dynamic re-planning in case the environmental situation changes, e.g. other traffic participants change their intention and the previously calculated trajectory does not guarantee safety anymore. Trajectories are described by polynomials and stored in look-up tables for different longitudinal velocities, longitudinal accelerations and maneuver duration times. Using a single-track model within a linear-quadratic control, the lateral deviation to the reference trajectory and the vehicle's orientation are controlled. The influence of parameter changes from additional payload, tire-road friction coefficients and tire properties on the vehicle-controller interaction are investigated with a sensitivity analysis on data generated with a simulation. The performance of the algorithm is presented and it is shown that many parameter variations will probably be perceived by occupants, but will not lead to safety-critical situations.

INDEX TERMS Automated driving, automated lane change, dynamic environments, dynamic re-planning, sensitivity analysis, trajectory planning.

I. INTRODUCTION

Automated lane changes are frequent maneuvers that have to be performed by automated vehicles in a safe and comfortable way in different traffic situations. According to [1], the three different levels of planning for automated driving include finding the best geometric path in a given traffic environment, realizing the best maneuver to perform in this traffic situation and finally designing the best trajectory. To achieve this, feasible trajectories have to be identified using environmental information such as position and relative velocity of other traffic vehicles as shown by [2], and road and/or lane geometry as shown by [3]. In previous studies, trajectories are often given as a four-dimensional state consisting of the longitudinal and lateral position of the ego vehicle, its heading angle and the road curvature as shown e.g. in [4]–[7]. To calculate these states, many researchers use predefined geometric curves like B-spline curves, see e.g. [8], or polynomials, see e.g. [9]. In this manner, the computational burden can be low enough to enable real-time capability.

The behavior of other traffic participants is often assumed to be static, e.g. keeping the current speed, or being predicted prior to initiation of the maneuver by identifying the intention of other traffic participants as shown in [10] and [11], or by only considering the risk that traffic participants on other lanes may pose, see [12] and [13]. Since a lane change maneuver endures several seconds and the intention of other traffic participants may change during this time period, dynamic re-planning ability is assumed to enhance safety. Recent studies pay attention to this issue. A method proposed by [2] enables re-planning in dynamic traffic environment that delivers a continuous and derivable re-planning trajectory that is feasible considering vehicle dynamics and road conditions. However, the optimum trajectory is chosen using differential evolution optimization method and suffers from high computational burden which is not suitable for real time applications. In [15], a real time trajectory re-planning for autonomous vehicle lane changes in uncertain traffic and a comfort-oriented strategy considering passenger demands

The associate editor coordinating the review of this manuscript and approving it for publication was Heng Wang.

is presented using an estimate of the driving status of surrounding vehicles. Speed, acceleration and jerk are controlled using Quadratic Programming with two separate controls for longitudinal and lateral direction. However, the dynamic equations of the vehicle are not considered, which may lead to deviations between controlled and planned trajectory in critical driving situations. In [16], a trajectory planning algorithm for lane change maneuvers based on mathematical functions is introduced. After choosing the appropriate trajectory, an algorithm for re-planning the lane change trajectory based on dynamic traffic conditions is proposed. Different mathematical functions for the trajectory are evaluated in terms of occupants' comfort. Artificial Bee Colony optimization is used to find the optimum lane, which does not allow real-time application in the implemented way. Liu *et al.* demonstrate an autonomous lane change decision-making model based on benefit, safety, and tolerance by analyzing the factors of the autonomous vehicle lane change. They apply a support vector machine algorithm with Bayesian Parameters Optimization to solve this problem, see [18]. The authors evaluate the performance using real vehicle data, however for comparably low speeds below 30 km/h. In [19], a planning model for a lane change under constraints of collision avoidance in dynamical driving environments is presented where longitudinal and lateral motion planning are decoupled. The longitudinal planning model decides a collision-free termination point of motion through planning the longitudinal acceleration and velocity. Taking the termination time as input, the lateral planning model plans the optimum reference trajectory for normal lane-changing maneuvers or re-plans the lane-changing trajectory to avoid imminent accidents. Dynamic stability is evaluated by comparing the acting horizontal acceleration with the friction circle for the current tire-road condition, without further specifying how information on the friction circle is made available.

In most driving situations, trajectories are desired to be comfortable for the occupants in terms of a smooth or jerk-free vehicle motion as shown by [11] and [20]. This can be ensured by choosing suitable mathematical or kinematic constraints for the given geometric path or by including a kinetic vehicle model. For the latter, linear single track models are often used which enable to ensure a stable vehicle response during the maneuver (e.g. limit side-slip angles, see [21] and [22]) and consider the maximum achievable acceleration dependent on the tire-road coefficient of friction, see [21] and [23]. However, in critical driving situations, a more aggressive maneuver may be required to avoid a collision. The most aggressive maneuver that still can be tracked depends on the vehicle's longitudinal speed, the vehicle's mass and the tire-road coefficient of friction as shown by [24]. An algorithm for the motion of a vehicle operating near the friction limits is given by [17]. They present a scheme that simultaneously modifies the desired trajectory and speed profile for a vehicle in response to the appearance of an obstacle, significant tracking error, or other environmental change. However, the vehicle and road parameters used may not be known accurately or may be subject to change, e.g. due to additional payload or on wet roads.

A recent overview on the characteristics of different lane change trajectory techniques is shown in [19], where real-time capability, computation cost and consideration of vehicle dynamics within the approaches are discussed. Their findings show that the existing approaches have significant shortcomings in at least one of these areas.

To overcome these shortcomings, we present an algorithm for an automated lane change that was developed with the aim to be computationally efficient for real-time capability and with the ability of re-planning the trajectory after maneuver initialisation in dynamic environments. The novelties compared to previous work from the authors, compare [2], [24] and [26], are:

- Real-time capable implementation of the algorithm with pre-stored look-up tables for feasible trajectories both for the initially planned one and the dynamic re-planning.
- An analysis of the effects on safety and the expected perception of occupants for the realistic case that vehicle parameters deviate during operation from the values assumed by the control.

The article is structured as follows: We start by describing the dynamic re-planning algorithm in Section II, which includes a description of the generation and choice of trajectories as well as the lateral control. In Section III, we show the performance of this algorithm: First for a typical over-taking maneuver and then for a critical driving situation that requires dynamic re-planning. Section IV investigates the influence of parameter changes on safety and the perceived vehicle motion. The focus lies on parameters that are subject to change during vehicle operation like the vehicle mass and the tire-road coefficient of friction.

All simulations have been performed with the real-time multi-body system software IPG CarMaker. The algorithm is also implemented in our driving simulator on the real-time processing unit XPACK4 from IPG Automotive GmbH. In this configuration, we reached triple real-time in different traffic scenarios. For a description of the driving simulator, see [27].

II. DESCRIPTION OF DYNAMIC LANE CHANGE SYSTEM

We present an algorithm for an automated lane change (LCA) that consists of two decision making units, the trajectory planning unit and the control unit, see Fig. 1. Re-planning is possible at certain points of the trajectory. The following iterative tasks are performed:

- **Decision Making I:** Using information on the tire-road friction coefficient, vehicle and traffic data, it is determined whether a safe lane change is possible. The number of lanes on the right and left side of the current vehicle lane are detected. When a lane change is desired either to the right or left lane and possible in a safe way,

the end point and maneuver time of the desired lane change maneuver are calculated.

- **Trajectory planning unit (Look-up table):** From an a-priori stored look-up table, trajectories are nominated that reach the desired end point during the desired maneuver time for the initial longitudinal velocity and for a pre-defined number of intermediary points. Since different longitudinal accelerations are possible during the maneuver, more than one trajectory is found.
- **Decision Making II:** The trajectory with the lowest lateral and longitudinal acceleration during the maneuver is chosen to consider occupants' comfort.
- **Traffic situation observation:** The vehicle's surroundings are observed using environmental sensors. In case there is a change in the traffic condition that requires an intervention to omit a collision, an iteration is started that allows to re-plan the trajectory dynamically at an intermediary point.
- **Control:** Using a single track model to consider the vehicle's behavior, the target values for steering angle, gas and brake pedal position are calculated.

The implementation of this algorithm is shown in [26].

A. GENERATION OF TRAJECTORIES

The lateral position $y(t)$ of the vehicle's trajectory during the lane change is described by [26] by the 5^{th} order polynomial

$$y(t) = a_5 \cdot t^5 + a_4 \cdot t^4 + a_3 \cdot t^3 + a_2 \cdot t^2 + a_1 \cdot t + a_0 \quad (1)$$

with the starting conditions

$$y(0) = \dot{y}(0) = \ddot{y}(0) = 0 \quad (2)$$

and the lateral offset $y(t_m) = \pm h$ at the end of the maneuver, with a negative value for a change to the right lane. At the end of the maneuver,

$$\dot{y}(t_m) = \ddot{y}(t_m) = 0. \quad (3)$$

For a lane change to the left, the lateral position can then be written as

$$y(t) = -\left(-\frac{6 \cdot h}{t_m^5} \cdot t^5 + \frac{15 \cdot h}{t_m^4} \cdot t^4 - \frac{10 \cdot h}{t_m^3} \cdot t^3\right), \quad (4)$$

see [26] for a detailed derivation of this formulation.

For a given lateral offset h, the lateral position over time mainly depends on the maneuver time t_m. The lateral acceleration $\ddot{y}$ also depends on t_m, where a decrease of t_m leads to increasing maximum lateral acceleration during the maneuver.

Different trajectories are calculated offline for different initial longitudinal velocities, longitudinal accelerations during the maneuver and maneuver times. The global optimization method *differential evolution* is used. Since this method is not real-time capable, it is used a-priori and the resulting trajectories are stored in a look-up table. Re-planning is only possible when reaching an intermediary point that has been stored before. For the present work, four intermediary points are stored for each lane change trajectory. Testing

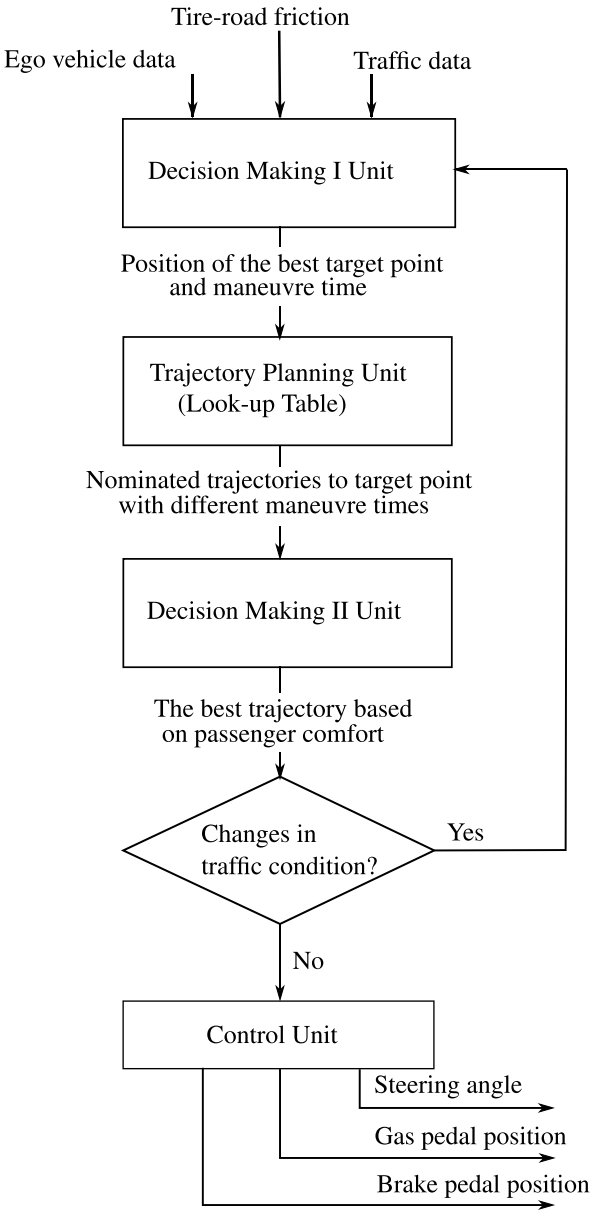

FIGURE 1. Structure of the automated lane change algorithm.

different scenarios, four intermediary points were a good compromise to avoid collisions in critical driving situation while still allowing an effective calculation time. The number of these intermediary points per trajectory is a measure for the flexibility in re-planning, but a too high number may yield to real-time issues during the search of suitable trajectories.

Fig. 2 shows the lateral position over time and four intermediary points additionally to start and end point for a lane change at an initial longitudinal velocity of 120 km/h. Fig. 3 shows the lateral position over the longitudinal position for different end points and longitudinal accelerations during the maneuver. The maneuver time varies between 4.5 and 6 s.

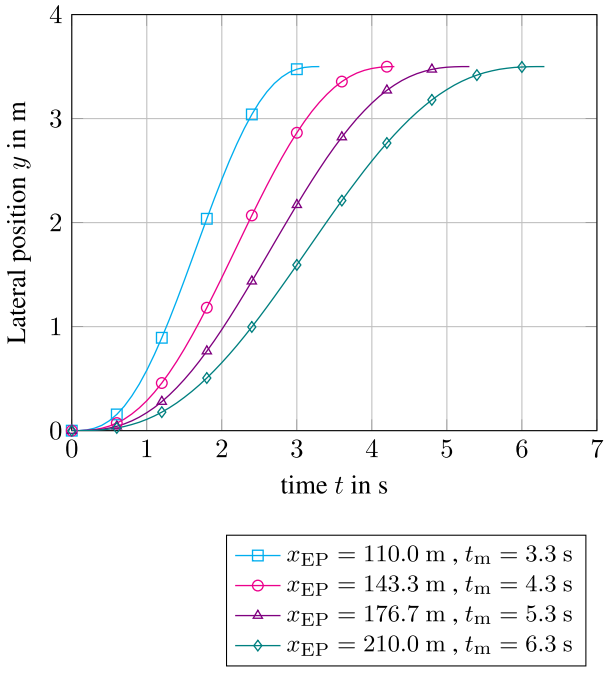

FIGURE 2. Lateral position over time for a lane change with different end points x_{EP} with start, end and four intermediary points for an initial velocity of 120 km/h.

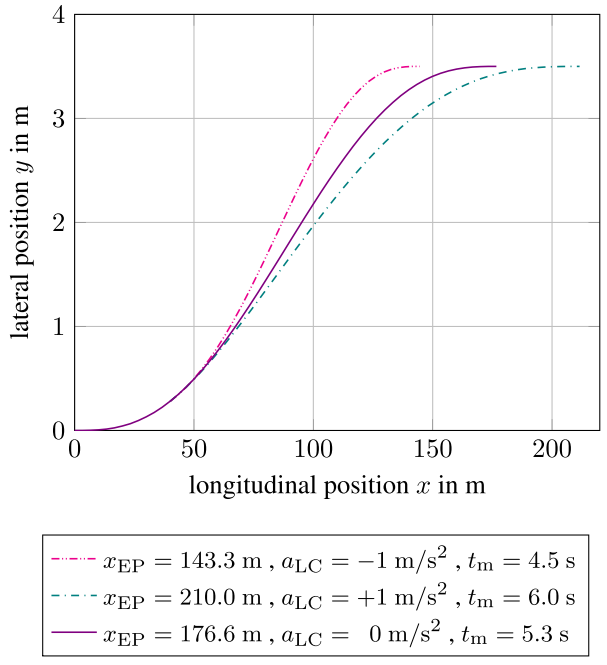

FIGURE 3. Lateral over longitudinal position during the lane change for different maneuver end points x_{EP} and longitudinal accelerations a_{LC} with the resulting maneuver times t_m.

B. LATERAL CONTROL FOR TRAJECTORY TRACKING

The lateral position is controlled using a linear-quadratic regulator (LQR) with four sub-models:

- A linear single-track model described by the state $\boldsymbol{x}_1 = \begin{bmatrix} v_y & \dot{\psi} \end{bmatrix}^{\mathrm{T}}$ with the lateral velocity v_y and the yaw rate $\dot{\psi}$ of the vehicle,

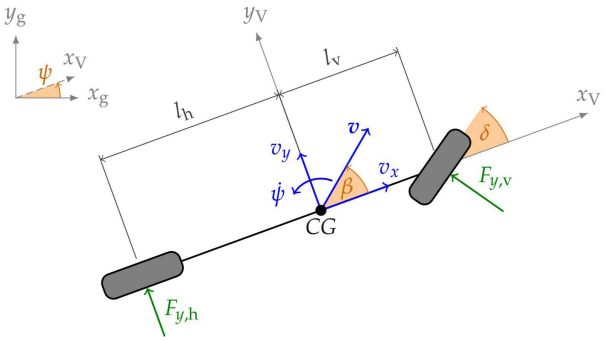

FIGURE 4. Kinematic and kinetic relations of the single-track model from [29].

- a dynamic model with the state $\boldsymbol{x}_2 = [y_L \quad \epsilon_L]$ including the relative lateral position y_L and the relative orientation angle ϵ_L to the planned trajectory,
- a dynamic steering model with the state $\boldsymbol{x}_3 = \begin{bmatrix} \delta_H & \dot{\delta}_H \end{bmatrix}$ with the steering angle δ_H and its time derivative and
- an integral action controller for the relative lateral position y_L to achieve stationary control accuracy described by $\boldsymbol{x}_4$.

The implementation is shown in [28]. The linear single-track model is given in the form

$$\dot{\boldsymbol{x}}_1 = \begin{bmatrix} -\dfrac{c_f + c_r}{m \cdot v_x} & \dfrac{-c_f \cdot l_f + c_r \cdot l_r}{m \cdot v_x} - v_x \\ \dfrac{-c_f \cdot l_f + c_r \cdot l_r}{I_z \cdot v_x} & -\dfrac{c_f \cdot l_f^2 + c_r \cdot l_r^2}{I_z \cdot v_x} \end{bmatrix} \boldsymbol{x}_1 + \begin{bmatrix} \dfrac{c_f}{m} \\ \dfrac{c_f \cdot l_f}{I_z} \end{bmatrix} \delta, \tag{5}$$

with c_f and c_r being the cornering stiffnesses of the front and rear tires, m the vehicle's mass, v_x the longitudinal velocity, l_f and l_r the longitudinal distances from the front and rear axle to the center of gravity (COG), I_z the vehicle yaw moment of inertia and δ the steering angle at the front wheels. The kinematic and kinetic relations of the single-track model are shown in Fig. 4.

The dynamics of the relative lateral position y_L and the relative orientation ϵ_L to the planned trajectory are considered by state $x_2 = [y_L \quad \epsilon_L]^{\mathrm{T}}$ and are given by

$$\dot{y}_L = v_x \cdot \epsilon_L - v_y - L \cdot \dot{\psi}, \tag{6}$$

$$\dot{\epsilon}_L = v_x \cdot \kappa_L - \dot{\psi}, \tag{7}$$

with L being the look-ahead distance and κ_L the curvature of the desired path, [30], [31]. The geometric relations are shown in Fig. 5.

The dynamic steering model is described by

$$\dot{\boldsymbol{x}}_3 = \begin{bmatrix} 0 & 1 \\ 0 & d_{gen} \end{bmatrix} \boldsymbol{x}_3 + \begin{bmatrix} 0 \\ \dfrac{i^2 \cdot V}{\zeta} \end{bmatrix} M_H + \begin{bmatrix} 0 & 0 \\ \dfrac{i}{\zeta} & -\dfrac{i}{\zeta} \end{bmatrix} \begin{bmatrix} F_l \\ F_r \end{bmatrix} \tag{8}$$

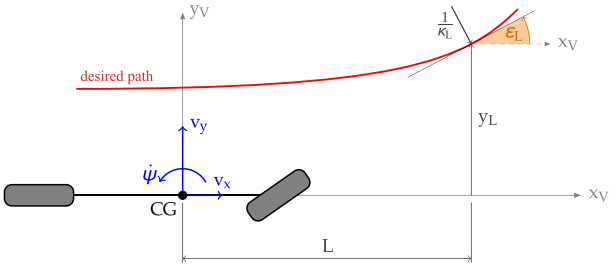

FIGURE 5. Dynamic model for the relative position of the vehicle to the planned trajectory described by the relative lateral position y_L and the relative orientation ϵ_L from [29].

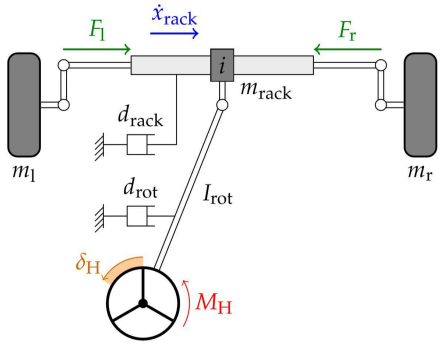

FIGURE 6. Dynamic steering model from [29].

with

$$\epsilon = m_l + m_r + m_{\text{rack}} + I_{\text{rot}} \cdot i^2, \tag{9}$$

$$d_{gen} = -\frac{1}{\epsilon}\left(d_{\text{rot}} \cdot i^2 + d_{\text{rack}}\right). \tag{10}$$

Therein, d_{rack} and d_{rot} are the damping coefficients of steering rack and the rotational steering components, $i = \delta_H \cdot x_{\text{rack}}$ the steering ratio between δ_H and rack position x_{rack}, V the amplification of the steering wheel torque M_H, F_l and F_r the tie road forces at the rack which have been modelled as disturbance variables, m_r and m_l the generalized masses of the left and right suspension, m_{rack} the steering rack mass and I_{rot} the moment of inertia of the rotating steering components. It is further assumed that the ratio α between the steering wheel angle δ_H and the wheel steering angle δ is constant. The dynamic steering model is described in [32] and shown in Fig. 6.

In the implementation of the algorithm, an integral action controller for the relative lateral position y_L is added to achieve the stationary control accuracy. For roads with higher permitted speeds like highways, clothoids are used as geometric functions for road design to enable smooth transitions. For a constant speed, the change of the radius in a clothoid curve results in a disturbance in form of a ramp on y_L, thus a two order integral with the additional state $\boldsymbol{x}_4$ is chosen in the form

$$\dot{\boldsymbol{x}}_4 = \begin{bmatrix} 0 & 1 \\ 0 & 0 \end{bmatrix} \boldsymbol{x}_4 + \begin{bmatrix} 0 \\ 1 \end{bmatrix} y_L. \tag{11}$$

Finally, the state space form of the overall controller model for the combined 8-dimensional state is given by

$$\boldsymbol{x} = [\boldsymbol{x}_1 \quad \boldsymbol{x}_2 \quad \boldsymbol{x}_3 \quad \boldsymbol{x}_4]^{\mathrm{T}} \tag{12}$$

$$= \begin{bmatrix} v_y & \dot{\psi} & y_L & \epsilon_L & \delta_H & \dot{\delta}_H & x_7 & x_8 \end{bmatrix}^{\mathrm{T}}, \tag{13}$$

$$\dot{\boldsymbol{x}} = \hat{\boldsymbol{A}} \cdot \boldsymbol{x} + \hat{\boldsymbol{b}} \cdot M_H + \hat{\boldsymbol{B}}_S \begin{bmatrix} \kappa_L \\ F_l \\ F_r \end{bmatrix}, \tag{14}$$

with system matrix of dimension 8×8 given by

$$\hat{\boldsymbol{A}} = \begin{bmatrix} a_{11} & a_{12} & 0 & 0 & \frac{c_f}{m \cdot \alpha} & 0 & 0 & 0 \\ a_{21} & a_{22} & 0 & 0 & \frac{c_f \cdot l_f}{I_z \cdot \alpha} & 0 & 0 & 0 \\ -1 & -L & 0 & v_x & 0 & 0 & 0 & 0 \\ 0 & -1 & 0 & 0 & 0 & 0 & 0 & 0 \\ 0 & 0 & 0 & 0 & 0 & 1 & 0 & 0 \\ 0 & 0 & 0 & 0 & 0 & a_{66} & 0 & 0 \\ 0 & 0 & 0 & 0 & 0 & 0 & 0 & 1 \\ 0 & 0 & 1 & 0 & 0 & 1 & 0 & 0 \end{bmatrix}, \tag{15}$$

with

$$a_{11} = \frac{c_f + c_r}{m \cdot v_x}, \tag{16}$$

$$a_{12} = -\frac{c_f \cdot l_f + c_r \cdot l_r}{m \cdot v_x} - v_x, \tag{17}$$

$$a_{21} = -\frac{c_f \cdot l_f + c_r \cdot l_r}{I_z \cdot v_x}, \tag{18}$$

$$a_{22} = -\frac{c_f \cdot l_f^2 + c_r \cdot l_r^2}{I_z \cdot v_x}, \tag{19}$$

$$a_{66} = \frac{1}{-\zeta}\left(d_{\text{rot}} \cdot i^2 + d_{\text{rack}}\right). \tag{20}$$

The input vector of dimension 8×1 is

$$\hat{\boldsymbol{b}} = \begin{bmatrix} 0 & 0 & 0 & 0 & 0 & \frac{i^2 \cdot V}{\zeta} & 0 & 0 \end{bmatrix}^{\mathrm{T}} \tag{21}$$

for input M_H and the disturbance matrix of dimension 8×3 is

$$\hat{\boldsymbol{B}}_S = \begin{bmatrix} 0 & 0 & 0 & v_x & 0 & 0 & 0 & 0 \\ 0 & 0 & 0 & 0 & 0 & \frac{1}{\epsilon} & 0 & 0 \\ 0 & 0 & 0 & 0 & 0 & -\frac{1}{\epsilon} & 0 & 0 \end{bmatrix}^{\mathrm{T}} \tag{22}$$

for disturbance input $\boldsymbol{x_S} = [\kappa_L \quad F_l \quad F_r]^{\mathrm{T}}$. Note that we treat κ_L as a disturbance and not a measurement. There are optical systems that deliver an estimate of the road curvature, however, there may be high deviations from the real curvature e.g. when the road marking quality is low.

The control law for $M_H = -\boldsymbol{k}^{\mathrm{T}}\boldsymbol{x}$ is determined by solving the quadratic optimization problem

$$J(M_H(t)) = \int_0^\infty \left(\boldsymbol{x}^{\mathrm{T}}(t) \cdot \boldsymbol{Q} \cdot \boldsymbol{x}(t) + R \cdot M_H^2\right)(d)t \tag{23}$$

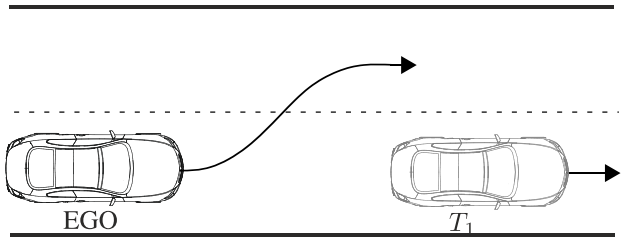

FIGURE 7. Scenario 1 - Ego vehicle with longitudinal speed of 130 km/h changes lane to overtake slower vehicle T_1 with 110 km/h.

with the weighing matrices $\boldsymbol{Q} = \boldsymbol{Q}^{\mathrm{T}} \geq 0$ and $R > 0$. Matrix $\boldsymbol{Q}$ is a diagonal matrix with the covariances of the states and the diagonal values were set to $\begin{bmatrix}0.1 & 0.1 & 10^6 & 0.1 & 0.1 & 0.1 & 100 & 100\end{bmatrix}$. These values were chosen in an iterative process with try and error. Since there is only one input, R is a scalar value and was set to 1 after examining the step response of the system.

III. RESULTS

The ability to plan and track trajectories for lane changes in dynamic environments will be shown using simulations in IPG CarMaker for different traffic situations. These situations include a typical overtaking maneuver as a standard case and a more complex situation that requires dynamic re-planning to omit an imminent collision. For the latter, a maneuver is chosen where a third vehicle is cutting in from the left after the ego vehicle started to overtake.

A. TRAJECTORY DURING OVERTAKING

A typical lane change maneuver is overtaking a slower vehicle T_1 on a multi-lane roadway as shown in Fig. 7. The performance of the planning and control algorithm is shown in the non-critical situation of the ego vehicle going with $v_x = 130$ km/h overtaking a slower target at $v_x = 110$ km/h on a road with lane width of 3.5 m. During this lane change, the algorithm adapts the longitudinal acceleration in a flexible way using the iterative structure in Fig. 1. This is compared to the trajectory for the pre-fixed maneuver time of 6.3 s, which is also the initial trajectory of the flexible trajectory. Fig. 8 shows the lateral position of the vehicle during a lane change. The maneuver is simulated with the flexible approach shown in Fig. 1. In this case, the trajectory is adapted 2 times during the maneuver. For comparison, the initially chosen trajectory is held constant without re-planning. In case of the flexible approach, the overall maneuver time is smaller. To show the performance of the control, we show the comparison of the planned lateral position y_P and the actual lateral position y as well as the tracking error $e_y = y_P - y$ in Fig. 9. Only the flexible approach is shown since it is the more challenging one for the control and shows higher tracking errors. The maximum absolute tracking error for this maneuver is 0.257 m.

Fig. 10 shows the lateral acceleration during the lane change maneuver for the flexible and the fixed lane change. The fixed lane change is very comfortable in terms of lateral

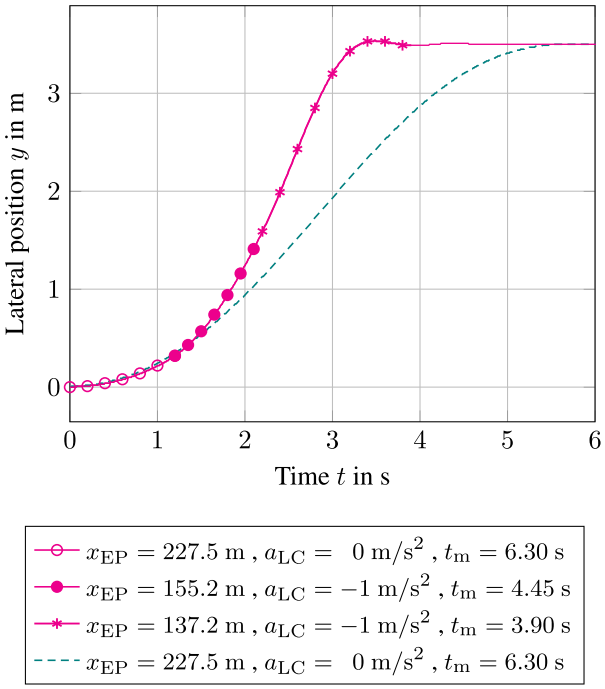

FIGURE 8. Scenario 1 - Lateral position during lane change for a flexible and a fixed maneuver time t_m. The flexible lane change consists of three different phases, where the first one is congruent with the fixed lane change.

acceleration and does not exceed ± 0.5 m/s^2. The flexible lane change has significant higher lateral accelerations of more than 3 m/s^2, which is due to the shorter maneuver time.

The lateral distance y_{lat} between the ego and the target vehicle during overtaking is shown in Fig. 11 for the flexible and the fixed lane change. In both simulations, the initial lateral distance is zero. During overtaking, this lateral distance increases and would reach 3.5 m in the final stage. However, once the ego vehicle has passed the target in longitudinal direction, it is not the relevant target anymore and the value goes back to 0 m before reaching the 3.5 m. Since the flexible lane change is finished before the ego vehicle is on the same longitudinal position in the driving direction as the target, the lateral distance does not change much. In the case of the fixed lane change, the smallest distance to the target vehicle is close to 0.1 m, representing a potential collision.

B. LANE CHANGES IN DYNAMIC ENVIRONMENTS

Overtaking can change into a critical situation when a third vehicle is cutting in from the left as shown in Fig. 12. Vehicle T_1 is driving with 110 km/h and the ego vehicle is approaching with 130 km/h. The calculated end point for a lane change to the second lane would be 155.2 m ahead of the ego vehicle and the maneuver time would be 4.3 s. However, shortly after initiating the lane change, a third vehicle approaches on the third lane and changes to the second lane. Without adaptation, a collision between ego vehicle and vehicle T_2 is imminent.

With the dynamic re-planning, a new end point for the maneuver is chosen 1.2 s after the lane change is initiated.

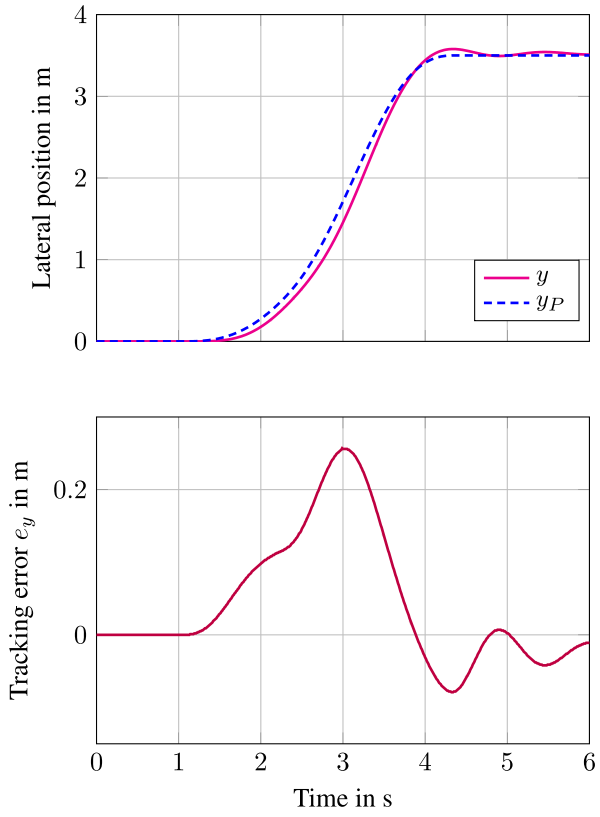

FIGURE 9. Scenario 1 - Planned lateral position y_P and actual lateral position y over time (above) as well as tracking error $e_y = y_P - y$ (below) for the automated lane change with the flexible maneuver time.

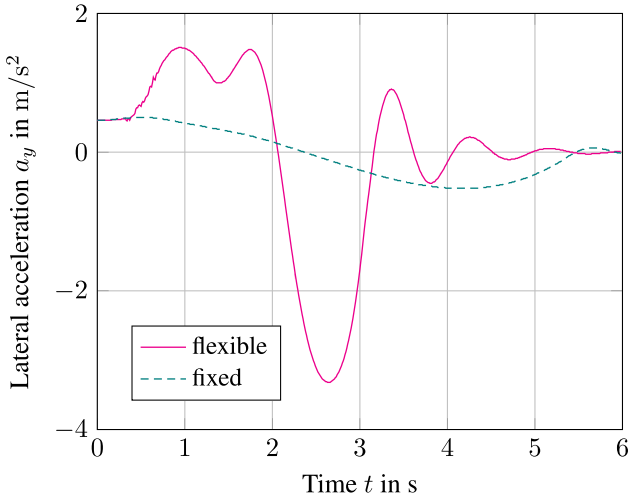

FIGURE 10. Scenario 1 - Lateral acceleration during lane change for a flexible and a fixed maneuver time.

A trajectory is automatically chosen where the ego vehicle constantly decreases with an acceleration of 1 m/s^2 in longitudinal direction and the collision is avoided.

Fig. 13 shows the lateral position over time for the initially planned and the dynamically re-planned trajectory. It is obvious that the re-planned trajectory has a shorter maneuver time due to the constant braking, which also results in higher

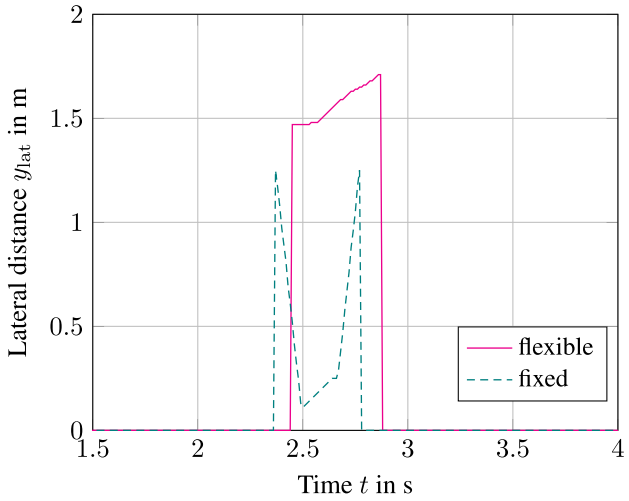

FIGURE 11. Scenario 1 - Lateral distance to overtaken traffic participant during lane change for a flexible and a fixed maneuver time.

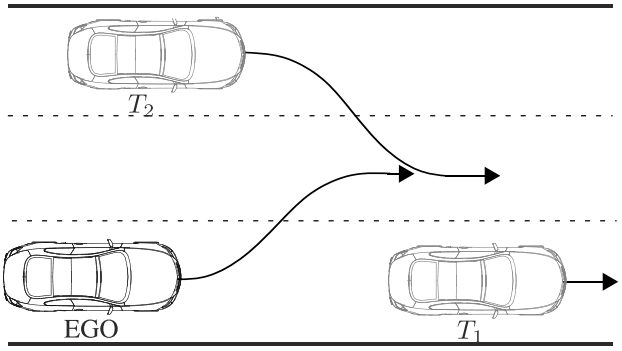

FIGURE 12. Scenario 2 - Ego vehicle with 130 km/h changes lane to overtake slower vehicle T_1 with 110 km/h, when suddenly vehicle T_2 cuts in from the left.

lateral accelerations as shown in Fig. 14. The longitudinal distance to vehicle T_2 is shown in Fig. 15. While there is a collision for the fixed maneuver time at about 39.5 s, the flexible lane change is not critical at any time. Again, the performance of the lateral control is shown by comparing the lateral planned position y_P and the actual lateral position y and the tracking error e_y in Fig. 16. The maximum lateral error for scenario 2 is 0.256 m.

IV. SENSITIVITY ANALYSIS

To achieve real-time capability and robustness of trajectory planning and tracking algorithms, the dynamic behaviour of the vehicle is simplified in these algorithms. These simplifications may lead to deviations between the predicted and the resulting ego vehicle behavior. In case they are too high, the control cannot follow the planned trajectory.

The focus of this analysis are dynamic vehicle parameters that are subject to change during vehicle operation either due to environmental influences or because they depend on the vehicle state itself. The following parameters are investigated:

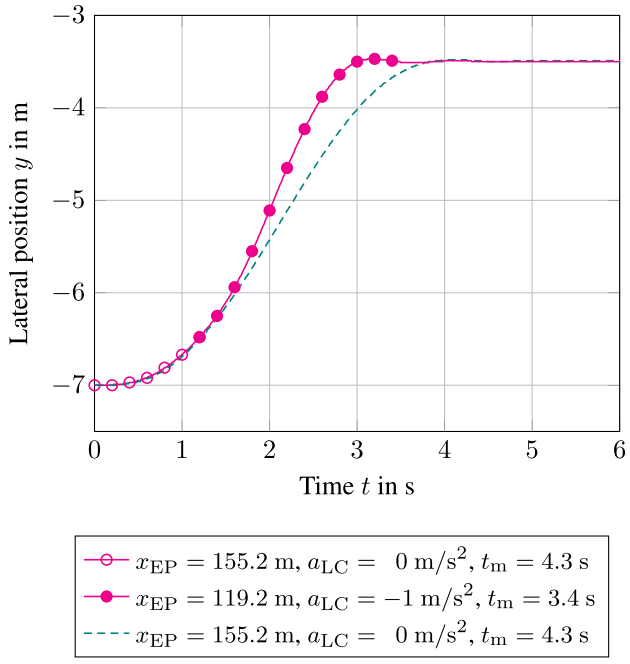

FIGURE 13. Scenario 2 - Lateral position over time for flexible and fixed maneuver time during overtaking maneuver with third vehicle cutting in from left.

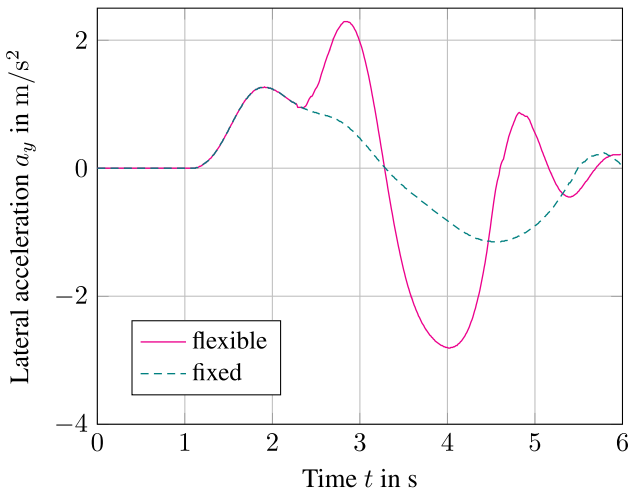

FIGURE 14. Scenario 2 - Lateral acceleration for flexible and fixed maneuver time during overtaking maneuver with third vehicle cutting in from left.

- **Tire-road friction coefficient (road condition):** This value may change depending on the properties and condition of the road, e.g. if there is presence of water, ice and snow, and the properties and conditions of the mounted tires. Typical values range from about 1.1 (high tire-road grip) to 0.1 (polished ice). Up to this day, there is no sensor available for series-production vehicles that has an detection accuracy that is good enough for safety-critical applications, see [37]. Thus this parameter cannot be assumed to be available as an input.

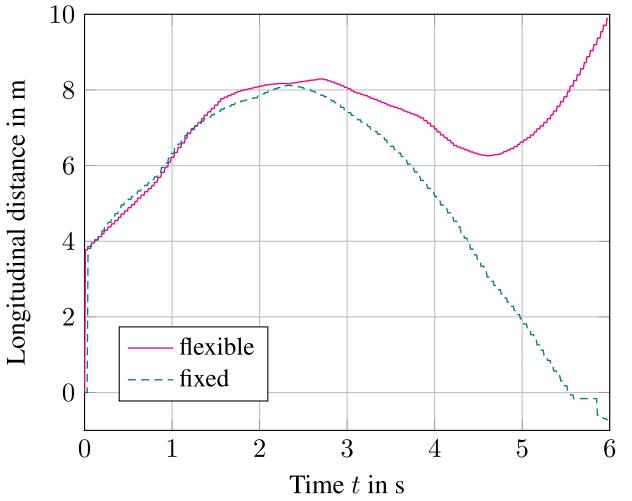

FIGURE 15. Scenario 2 - Longitudinal distance to target vehicle T_2 during overtaking maneuver with third vehicle cutting in from left.

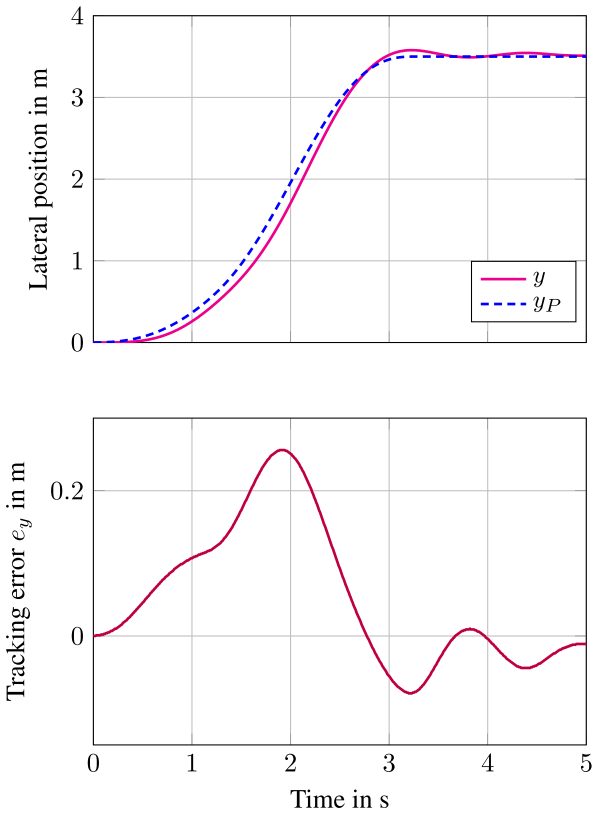

FIGURE 16. Scenario 2 - Planned lateral position y_P and actual lateral position y over time (above) as well as tracking error $e_Y = y_P - y$ (below) for the automated lane change with the flexible maneuver time.

- **Vehicle mass m and location of the center of gravity:** The vehicle mass varies depending on number of occupants and payload. These additional masses can be arranged in the vehicle within certain limitations, leading to different horizontal and vertical positions of the center of gravity and may influence the vehicle's steering tendency, among others.

TABLE 1. Parameters, their ranges for the variation and the reference values.

Parameter	Variation	Reference value
μ	0.1:0.1:0.9	0.9
c_f	0.8:0.05:1.2 $\cdot c_{f,ref}$	$c_{f,ref}$ = 140.000 N/rad
c_r	0.8:0.05:1.2 $\cdot c_{f,ref}$	$c_{r,ref}$ = 140.000 N/rad
m	1560:100:2260 kg	1560 kg
x_{COG}	2:0.05:2.9 m	2.6 m
z_{COG}	0.6:0.05:0.85 m	0.6 m

- **Tire's cornering stiffnesses front c_f and rear c_r:** Constant cornering stiffnesses hold for operations in the linear region of the tire and when there is no vertical load transfer. The non-linear region of the tire typically starts at lateral accelerations from 3 to 4 m/s^2, which is not exceeded during the maneuvers.
- **Lateral velocity estimate:** This input is required for the presented observer. For series-production applications, no direct measurement but observers are used to determine the lateral velocity v_y or the related side-slip angle β.
- **Tire's lateral force estimates (front and rear):** Like v_y, observers are typically used to determine the current lateral tire forces for series-production applications. In the linear tire region, the forces can be described by c_f and c_r, thus a deviation will have an influence comparable to these parameter variations and thus the influences of lateral force estimates is not investigated separately.

Hence, a sensitivity analysis was performed with the parameter variations shown in Table 1. Typical values of these parameters are chosen that can occur during vehicle operation, not considering misuse. The longitudinal position x of the COG is defined as the distance from the rear outside edge of vehicle to the COG in longitudinal direction. The reference value is the value for a weight distribution of 50% on the front and the rear axle. The vertical position z of the COG is defined as the distance from the even road surface to the COG.

The influence of these parameters on the resulting vehicle reaction in interaction with the control is of interest. In the following study, vehicle states and control inputs are investigated that are related to either:

- comfort of occupants (namely the states a_x, a_y and $\dot{\psi}$),
- objective safety, which is compromised when either the lane markings are crossed unintentionally during the maneuver which may lead to a collision, or when the vehicle state is not stable. These two situations are described by states y_L and v_y. Except for low friction surfaces below $\mu > 0.3$ where the physical limits were exceeded, the lane markings were never crossed in any of the simulations. Concerning vehicle stability, in the development of Electronic Stability Control it was considered by [36] that average drivers do not exceed slip angles β of ± 2 deg. Considering the relation $\beta = \tan^{-1}\left(v_y/v_x\right)$, we see that there were no unstable vehicle states in the simulations except those on $\mu > 0.3$.

Having ruled out objectively unsafe situations, a description of the used comfort-related thresholds is given in the following and the values used for this study are summarized in Table 2.

1) COMFORT-RELATED THRESHOLDS

Humans show a response threshold from which a certain excitation level can be perceived and a different threshold to detect changes in an existing excitation as described by [33, p. 32]. During driving, the two translational accelerations a_x and a_y and the rotational acceleration $\dot{\psi}$ are mainly perceived. We assume that in order to have high values of comfort of occupants, the deviation in these accelerations due to parameter changes shall be not perceivable or small. Thresholds from literature will be discussed and selected values described. Since these thresholds are based on statistical evaluations, they will differ from person to person according to [33, p. 32].

In longitudinal direction, the human perception threshold shows a high range for a_x from 0.02 to 0.8 m/s^2 according to [34]. Although not necessarily perceived as uncomfortable, we assume that occupants will notice a difference of $a_{x,th} = 0.4$ m/s^2, which is about the mean value of [34].

In lateral direction, [34] gives a range from 0.05 to 0.1 m/s^2 for different test scenarios. For this study, the higher value of $a_{y,th} = 0.1$ m/s^2 is chosen.

While accelerations are detected with the vestibular system, humans perceive rotational velocities like the yaw rate with visual information as described by [33, p. 34]. A perception threshold value $\dot{\psi}_{th} = 0.0017$ rad/s (0.1 deg/s) is given by [35] and used here.

2) SENSITIVITY RESULTS

Table 2 shows the minimum and maximum deviations from the respective property simulated with the parameter reference. For all parameters, it is noted with asterisks (*) if the perception threshold is not crossed by any parameter variation. We differentiate in μ high for coefficients of friction $\mu \geq 0.3$ and μ low, since for the latter the vehicle is at the physical limits and the control cannot track the planned trajectory. The highest influences are seen for parameter variations of m and μ, being followed by the rear tire stiffness c_r and the vertical position z_{COG}.

Fig. 17 shows the maximum absolute deviation between simulations with a specific set parameter to the reference simulation for the main influences μ, m, c_r and z on the vehicle states a_y. The deviations of a_y increase with increasing parameter value for m and c_r, decrease for increasing μ and show a minimum at the reference for c_r. Mass and c_r show the highest deviations. The same tendency can be seen in Fig. 18 for the influence of these parameters on $\dot{\psi}$.

The relative lateral position y_L during the lane change is shown in Fig. 19 for the reference simulation, the maximum

TABLE 2. Maximum and minimum values of states for parameter variations and perception threshold.

Parameters	a_x (0.4 m/s^2)	a_y (0.1 m/s^2)	$\dot{\psi}$ (0.002 rad/s)
μ low	-1.75, 2.18	-3.72, 2.94	-47.51, 51.22
μ high	-1.02, 1.07	-0.46, 0.42	-1.22, 0.8
m	-0.54, 0.7	-1.65, 1.31	-2.97, 2.21
c_f	$\pm$ 0.05*	$\pm$ 0.05*	$\pm$ 0.12
c_r	-0.05*, 0.09*	-0.28, 0.29	-0.89, 1.14
x_{COG}	$\pm$ 0.26*	-0.34,0.25	-0.26, 0.18
z_{COG}	-0.1*, 0.15*	-0.29, 0.28	-0.4, 0.56

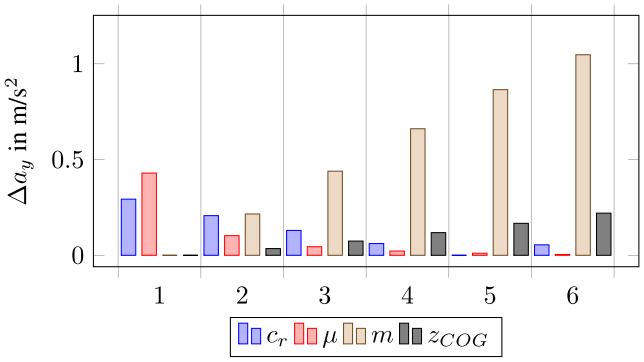

FIGURE 17. Maximum of absolute deviation of a_y for parameter variations of c_r, μ, m and z_{COG}. For c_r and m, the first six parameter variations are shown.

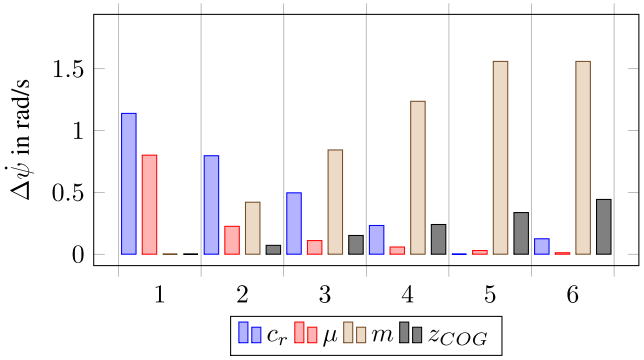

FIGURE 18. Maximum of absolute deviation of the yaw rate for all parameter variations of c_r, μ, m and z_{COG}. For c_r and m, the first six parameter variations are shown.

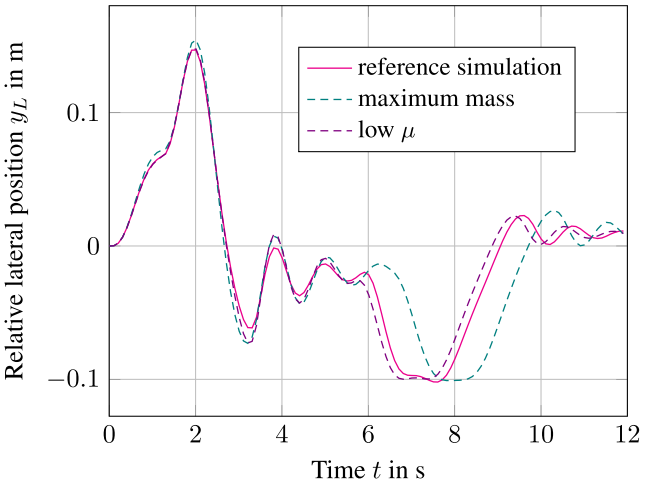

FIGURE 19. Relative lateral position y_L for the reference simulation (μ = 0.9, m = 1560 kg and z_{COG} = 0.6 m), for the maximum mass (m = 2260 kg) and a low coefficient of friction (μ = 0.3).

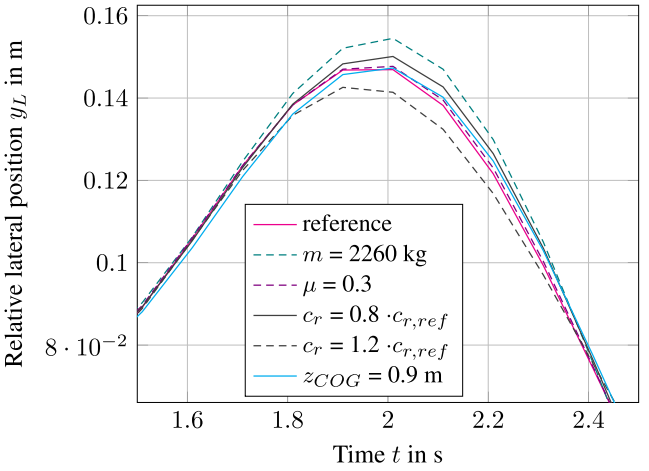

FIGURE 20. Relative lateral position y_L for the reference simulation (μ = 0.9, m = 1560 kg and z_{COG} = 0.6 m) and for the following corner cases for the time between 1.5 and 2.5 s: Maximum mass (m = 2260 kg), low coefficient of friction (μ = 0.3), 80% and 120% of the reference cornering stiffness for the rear wheels and a high center of gravity (z_{COG} = 0.9 m).

mass of 2260 kg and a low coefficient of friction $\mu = 0.3$. In all simulations, the highest deviations was achieved for the maximum mass variation $m = 2260$ kg, both in terms of different amplitude and a phase shift due to the higher inertial resistance of the vehicle.

Fig. 20 and Fig. 21 show details from Fig. 19 for selected time spans. Other than in Fig. 19, additional corner cases from parameter variations are shown. These include the highest influences seen in all simulations, namely from the rear cornering stiffness which was varied between 80 and 120%, and the height of the COG with the maximum at $z_{COG} = 0.9$ m.

Fig. 22 shows the lateral acceleration for the reference simulation, the maximum mass and the low friction value. Again, the vehicle mass shows the highest difference in amplitudes and phase shift. A detailed look on the time span from 2.5 to 4.5 s is given in Fig. 23, again with additional corner cases. Similar to Fig. 21, the parameter variations show a comparable tendency towards the reference curve concerning the lateral accelerations.

It can be seen that with the exception of μ low situations, the algorithm is insensitive to the investigated parameters and leads to small deviations when examining the lateral position compared to the planned trajectory and the resulting changes in lateral acceleration. For corner cases of the variations of vehicle mass, the coefficient of friction, the rear cornering stiffness and the height of the vehicle's center of gravity, the assumed perception thresholds are exceeded, especially of the yaw rate.

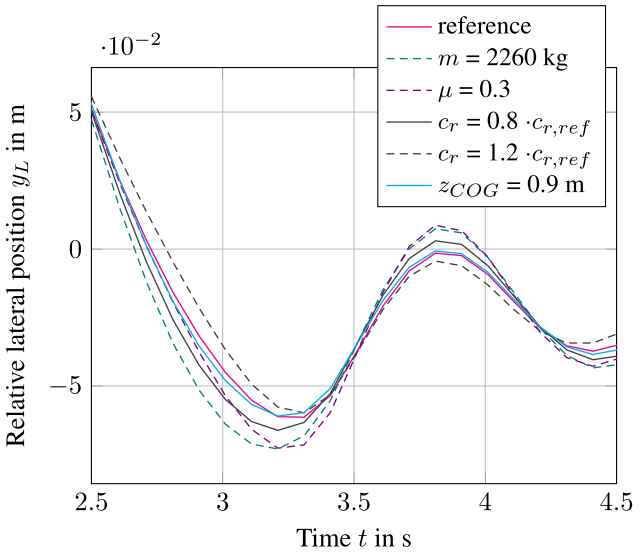

FIGURE 21. Relative lateral position y_L for the reference simulation (μ = 0.9, m = 1560 kg and z_{COG} = 0.6 m) and for the following corner cases for the time between 2.5 and 4.5 s: Maximum mass (m = 2260 kg), low coefficient of friction (μ = 0.3), 80% and 120% of the reference cornering stiffness for the rear wheels and a high center of gravity (z_{COG} = 0.9 m).

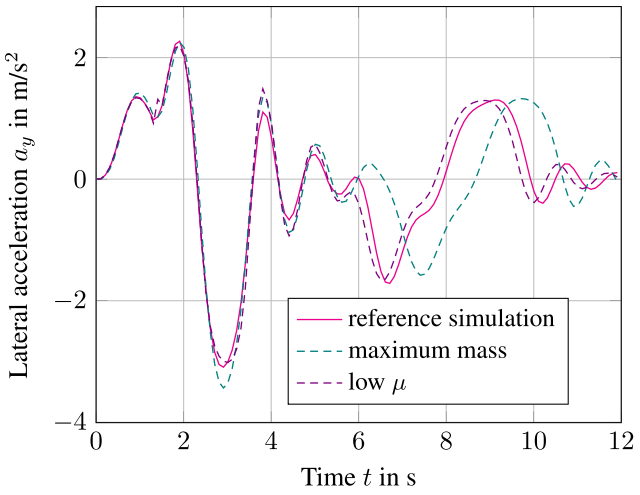

FIGURE 22. Lateral acceleration a_y for the reference simulation (μ = 0.9, m = 1560 kg and z_{COG} = 0.6 m), for the maximum mass (m = 2260 kg) and a low coefficient of friction (μ = 0.3).

The influence of these parameters can be minimized for future work by using real-time estimates as an input to the automated lane change algorithm. According to [38], the tasks of vehicle dynamic state estimation include estimation of motion variables of vehicle body, axle and/or wheels such as the vehicle speed over ground, vehicle parameters such as the vehicle mass and environmental variables like the tire-road friction. By considering these estimates, the vehicle's dynamic response can be adapted adequately. A comprehensive state of the art on vehicle dynamic state estimation is given in [39].

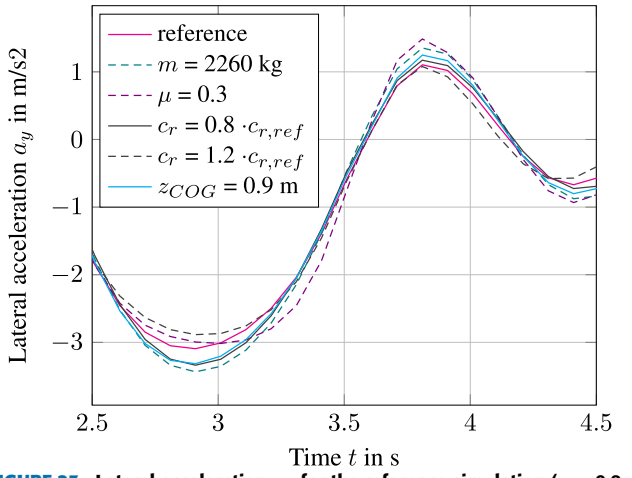

FIGURE 23. Lateral acceleration a_y for the reference simulation (μ = 0.9, m = 1560 kg and z_{COG} = 0.6 m) and for the following corner cases for the time between 2.5 and 4.5 s: Maximum mass (m = 2260 kg), low coefficient of friction (μ = 0.3), 80% and 120% of the reference cornering stiffness for the rear wheels and a high center of gravity (z_{COG} = 0.9 m).

V. CONCLUSION

An algorithm for an automated lane change is presented that is able to perform re-planning of the trajectory in changing dynamic environments, e.g. due to change of intention of other traffic occupants that leads to critical situations without intervention. The lateral position of the vehicle's trajectory is described by a polynomial of order 5. A linear-quadratic regulator is used to control the deviation of the lateral position. Within this controller, a linear single-track model and a dynamic steering model are used to consider a realistic vehicle behaviour. Re-planning can be performed at predefined points of the calculated trajectory.

The performance of the algorithm is shown for different maneuver end points and longitudinal accelerations. The difference between fixed and flexible maneuver end time is shown for the resulting lateral distance of the vehicle to the lane, the lateral acceleration and the lateral distance to other traffic occupants. It is also shown that the re-planning algorithm is able to avoid a collision for an overtaking maneuver in progress, with a third vehicle suddenly cutting in from the left lane.

Vehicle and road parameters may vary during operation and will influence the vehicle-controller-interaction. A sensitivity analysis is performed to show the influence of payload changes (e.g. mass and its location), the tire-road coefficient of friction and the tire properties front and rear cornering stiffness on the vehicle's response. It is shown that for typical parameter variations, the lateral position of the vehicle and the vehicle's side-slip angle are within safety-related thresholds. However, some variations are likely to be perceived by occupants and may lead to decreasing levels of comfort and subjective safety by the users.

Overall, it is shown that a safe automated lane change is possible in changing dynamic environments which is also safe in terms of parameter variations of vehicle and road.

ACKNOWLEDGMENT

The authors would like to thank the former master students A. Glibusic and G. Nestlinger who were involved in the implementation and validation in IPG CarMaker of the presented work.

REFERENCES

[1] C. Katrakazas, M. Quddus, W.-H. Chen, and L. Deka, "Real-time motion planning methods for autonomous on-road driving: State-of-the-art and future research directions," *Transp. Res. C, Emerg. Technol.*, vol. 60, pp. 416–442, Nov. 2015.

[2] S. Samiee, A. Eichberger, S. Azadi, and R. Kazemi, "A novel approach for a collision avoiding lane change system in a dynamic traffic environment," in *Proc. Dyn. Veh. Roads Tracks (IAVSD)*, Graz, Austria, Aug. 2015, pp. 237–242.

[3] V. Leonhardt and G. Wanielik, "Feature evaluation for lane change prediction based on driving situation and driver behavior," in *Proc. 20th Int. Conf. Inf. Fusion (Fusion)*, Xi'an, China, Jul. 2017, pp. 1–7.

[4] M. Pivtoraiko and A. Kelly, "Efficient constrained path planning via search in state lattices," in *Proc. 8th Int. Symp. Artif. Intell., Robot. Automat. Space*, Munich, Germany, Sep. 2005, pp. 1–7.

[5] J. Schröder, T. Gindele, D. Jagszent, and R. Dillmann, "Path planning for cognitive vehicles using risk maps," in *Proc. IEEE Intell. Veh. Symp. (IV)*, Einhoven, The Netherlands, Jun. 2008, pp. 1119–1124.

[6] M. C. D. J. M. McNaughton Urmson and J.-W. Lee, "Motion planning for autonomous driving with a conformal spatiotemporal lattice," in *Proc. IEEE Int. Conf. Robot. Autom. (ICRA)*, Shanghai, China, May 2011, pp. 4889–4895.

[7] I. Bae, J. H. Kim, and S. Kim, "Steering rate controller based on curvature of trajectory for autonomous driving vehicles," in *Proc. IEEE Intell. Veh. Symp. (IV)*, Gold Coast, QLD, Australia, Jun. 2013, pp. 1381–1386.

[8] X. Li, Z. Sun, D. Cao, Z. He, and Q. Zhu, "Real-time trajectory planning for autonomous urban driving: Framework, algorithms, and verifications," *IEEE/ASME Trans. Mechatronics*, vol. 21, no. 2, pp. 740–753, Apr. 2016.

[9] F. You, R. Zhang, G. Lie, H. Wang, H. Wen, and J. Xu, "Trajectory planning and tracking control for autonomous lane change maneuver based on the cooperative vehicle infrastructure system," *Expert Syst. Appl.*, vol. 42, no. 14, pp. 5932–5946, Aug. 2015.

[10] V. Leonhardt, T. Pech, and G. Wanielik, "Data fusion and assessment for maneuver prediction including driving situation and driver behavior," in *Proc. 19th Int. Conf. Inf. Fusion*, Heidelberg, Germany, Jul. 2016, pp. 1702–1708.

[11] R. Solea and U. Nunes, "Trajectory planning with velocity planner for fully-automated passenger vehicles," in *Proc. IEEE Intell. Transp. Syst. Conf.*, Toronto, ON, Canada, Sep. 2006, pp. 474–480.

[12] B. Vanholme, S. Glaser, S. Mammar, and D. Gruyer, "Manoeuvre-based trajectory planning for highly autonomous vehicles on real road with traffic," in *Proc. Eur. Control Conf. (ECC)*, Hungary, Budapest, Aug. 2009, pp. 3281–3286.

[13] W. Yao, H. Zhao, P. Bonnifait, and H. Zha, "Lane change trajectory prediction by using recorded human driving data," in *Proc. IEEE Intell. Veh. Symp. (IV)*, Gold Coast, QLD, Australia, Jun. 2013, pp. 430–436.

[14] X. Hu, L. Chen, B. Tang, D. Cao, and H. He, "Dynamic path planning for autonomous driving on various roads with avoidance of static and moving obstacles," *Mech. Syst. Signal Process.*, vol. 100, pp. 482–500, Feb. 2018.

[15] B. Qiao and X. Wu, "Real time trajectory re-planning for autonomous vehicle lane changing in uncertain traffic," in *Proc. IEEE 28th Int. Symp. Ind. Electron. (ISIE)*, Vancouver, BC, Canada, Jun. 2019, pp. 1524–1529.

[16] A. Norouzi, R. Kazemi, and O. Abbasi, "Path planning and re-planning of lane change manoeuvres in dynamic traffic environments," *Int. J. Veh. Auton. Syst.*, vol. 14, no. 3, pp. 239–264, 2019.

[17] J. K. Subosits and J. C. Gerdes, "From the racetrack to the road: Real-time trajectory replanning for autonomous driving," *IEEE Trans. Intell. Veh.*, vol. 4, no. 2, pp. 309–320, Jun. 2019.

[18] Y. Liu, X. Wang, L. Li, S. Cheng, and Z. Chen, "A novel lane change decision-making model of autonomous vehicle based on support vector machine," *IEEE Access*, vol. 7, pp. 26543–26550, 2019.

[19] H. Zheng, J. Zhou, Q. Shao, and Y. Wang, "Investigation of a longitudinal and lateral lane-changing motion planning model for intelligent vehicles in dynamical driving environments," *IEEE Access*, vol. 7, pp. 44783–44802, 2019.

[20] J. Feng, J. Ruan, and Y. Li, "Study on intelligent vehicle lane change path planning and control simulation," in *Proc. IEEE Int. Conf. Inf. Acquisition*, Weihai, China, Aug. 2006, pp. 683–688.

[21] D. Madas, M. Nosratinia, M. Keshavarz, P. Sundstrom, R. Philippsen, A. Eidehall, and K.-M. Dahlen, "On path planning methods for automotive collision avoidance," in *Proc. IEEE Intell. Veh. Symp. (IV)*, Gold Coast, QLD, Australia, Jun. 2013, pp. 931–937.

[22] I. Bae, J. Moon, H. Park, J. Kim, and S. Kim, "Path generation and tracking based on a Bezier curve for a steering rate controller of autonomous vehicles," in *Proc. IEEE Conf. Intell. Transp. Syst. (ITSC)*, The Hague, The Netherlands, Oct. 2013, pp. 436–441.

[23] O. Sawodny, J. Zimmermann, and A. Lutz, "Motion planning for an autonomous vehicle driving on motorways by using flatness properties," in *Proc. IEEE Int. Conf. Control Appl.*, Yokohama, Japan, Sep. 2010, pp. 908–913.

[24] S. Samiee, L. Shao, B. Rogic, A. Eichberger, S. Azadi, and R. Kazemi, "A comprehensive algorithm for automatic emergency lane-change," in *Proc. Dyn. Veh. Roads Tracks (IAVSD)*, Rockhampton, QLD, Australia, Aug. 2017, pp. 353–358.

[25] A. Glibusic, "Implementierung von dynamischer Trajektorienplanung beim automatisierten Fahrstreifenwechsel in eine virtuelle Testumgebung," M.S. thesis, Dept. Inst. Automot. Eng., Graz Univ. Technol., Graz, Austria, 2019.

[26] S. Samiee, S. Azadi, R. Kazemi, and A. Eichberger, "Towards a decision-making algorithm for automatic lane change manoeuvre considering traffic dynamics," *PROMET-Traffic&Transportation*, vol. 28, no. 2, pp. 91–103, Apr. 2016.

[27] S. Arefnezhad, A. Eichberger, M. Frühwirth, C. Kaufmann, M. Moser, and I. V. Koglbauer, "Driver monitoring of automated vehicles by classification of driver drowsiness using a deep convolutional neural network trained by scalograms of ECG signals," *Energies*, vol. 15, no. 2, p. 480, Jan. 2022.

[28] G. Nestlinger, "Modellbildung und Simulation eines Spurhalte-Assistenzsystems," M.S. thesis, Dept. Inst. Automat. Control, Graz Univ. Technol., Graz, Austria, 2013.

[29] G. Nestlinger and M. Stolz, "Bumpless transfer for convenient lateral car control handover," *IFAC-PapersOnLine*, vol. 49, no. 15, 2016, pp. 132–138.

[30] J. Kosecka, R. Blasi, C. J. Taylor, and J. Malik, "A comparative study of vision-based lateral control strategies for autonomous highway driving," in *Proc. IEEE Int. Conf. Robot. Autom.*, May 2018, pp. 1903–1908.

[31] J. Kosecka, R. Blasi, C. J. Taylor, and J. Malik, "Vision-based lateral control of vehicles," in *Proc. IEEE Conf. Intell. Transp. Syst.*, Nov. 1997, pp. 900–905.

[32] *CarMaker Reference Manual*, Version 7.1.1, IPG Automotive GmbH, Karlsruhe, Germany, 2018.

[33] A. Lange, "Gestaltung der Fahrdynamik beim Fahrstreifenwechselmanöver als Rückmeldung für den Fahrer beim automatisierten Fahren," Ph.D. dissertation, Dept. Chair Ergonom., Tech. Univ. Munich, Munich, Germany, 2017.

[34] B. Heißing, D. Kudritzki, R. Schindlmaister, and G. Mauter, "Menschengerechte Auslegung des dynamischen Verhaltens von PKW," in *Ergonomie und Verkehrssicherheit*, H. Bubb, Ed. Munich: Herbert Utz Verlag, 2000.

[35] Y. Muragishi, K. Fukui, and E. Ono, "Development of a human sensitivity evaluation system for vehicle dynamics," *AutoTechnology*, vol. 7, no. 6, pp. 56–58, 2007.

[36] A. T. van Zanten, "Bosch ESP systems: 5 years of experience," SAE Tech. Paper 2000-01-1633, 2000, pp. 211–220.

[37] A. Tuononen, M. Ovaska, and A. Niskanen, "Review on tire-road-friction potential estimation technologies," in *Proc. Dyn. Veh. Roads Tracks (IAVSD)*, Gothenburg, Sweden, Aug. 2019, pp. 1027–1032.

[38] M. Klomp, M. Jonasson, L. Laine, L. Henderson, E. Regolin, and S. Schumi, "Trends in vehicle motion control for automated driving on public roads," *Veh. Syst. Dyn.*, vol. 57, no. 7, pp. 1028–1061, Jul. 2019.

[39] H. Guo, D. Cao, H. Chen, C. Lv, H. Wang, and S. Yang, "Vehicle dynamic state estimation: State of the art schemes and perspectives," in *IEEE/CAA J. Automatica Sinica*, vol. 5, no. 2, pp. 418–431, Feb. 2018.

CORNELIA LEX received the Diploma degree (equivalent to the M.Sc. degree) in mechanical engineering and the Ph.D. degree from the Graz University of Technology, Austria, in 2008 and 2015, respectively. From 2008 to 2017, she was a Research Assistant with the Institute of Automotive Engineering, Graz University of Technology. Since 2017, she has been holding an assistant professor position with a tenure track. She is currently the Head of the working group 'Vehicle Dynamics & Tires', the workshop and the suspension and brake test bench at the Institute of Automotive Engineering at TU Graz. Her research interests include vehicle motion state estimation and tire-road state estimation for automated driving and vehicle dynamics in simulation and modeling, especially tire modeling and testing.

DEMIN NALIC (Member, IEEE) received the bachelor's degree in electrical engineering and information technologies and the master's degree in control and automation engineering from the Vienna University of Technology, in 2015 and 2016, respectively. He was a Software Engineer and the Project Leader for smart manufacturing at Siemens, Austria, from 2016 to 2018. Since 2019, he has been within the IEEE Member of the Intelligent Transportation Systems and Vehicular Technology Society. He is currently working as a Research Assistant with the Institute of Automotive Engineering, Graz University of Technology. His research interests include autonomous systems, testing methodologies, and control solutions for automated driving systems.

SAJJAD SAMIEE received the master's degree in mechanical engineering and the Ph.D. degree in the field of dynamics and control from the K. N. Toosi University of Technology, Teheran, in 2008 and 2016, respectively. In 2013, he joined the Institute of Automotive Engineering, Graz University of Technology, as a Visiting Researcher, and then started working there as a Research Assistant. After receiving his Ph.D. degree, he continued his postdoctoral study for three more years there. His research interests include vehicle dynamics and control with the application in advanced driver assistance systems and autonomous vehicles.

ARNO EICHBERGER received the degree in mechanical engineering from the University of Technology Graz, in 1995, and the Ph.D. degree in technical sciences, in 1998. From 1998 to 2007, he was employed at MAGNA STEYR Fahrzeugtechnik AG&Co and dealt with different aspects of active and passive safety. Since 2007, he has been working with the Institute of Automotive Engineering, University of Technology Graz, dealing with driver assistance systems, vehicle dynamics, and suspensions. Since 2012, he has been an Associate Professor holding a venia docendi of automotive engineering.